

possible that B61 may also be responsible in part for the angiogenic activities of other proinflammatory factors.

## REFERENCES AND NOTES

1. L. B. Holzman, R. M. Marks, V. M. Dixit, *Mol. Cell. Biol.* **10**, 5830 (1990).
2. H. Shao, A. Pandey, M. Seldin, K. S. O'Shea, V. M. Dixit, *J. Biol. Chem.* **270**, 5636 (1995).
3. The B61-Ig chimera was made with the following primers generated by polymerase chain reaction: 5' primer with a custom Nhe I site (underlined), CCG CCG CTA GCT GAT CGC CAC ACC GTC TTC TGG AAC AGT, and a 3' primer with a Bam HI site (underlined), CTC GGG ATC CCT GTG ACC GAT GCT ATG TAG AAC CCG CAC. The control-Ig chimera was made as described (19). The amplified fragments were digested and cloned into Nhe I- and Bam HI-cut CD5-IgG1 vector [A. Aruffo, I. Stamenkovic, M. Melnick, C. B. Underhill, B. Seed, *Cell* **61**, 1303 (1990)]. The Ig chimeras were purified from pooled supernatants of transfected 293T cells as described (19).
4. T. D. Bartley *et al.*, *Nature* **368**, 558 (1994).
5. A. Pandey, R. M. Marks, P. J. Polverini, V. M. Dixit, unpublished data.
6. HUVECs were grown in 2% fetal bovine serum (FBS) without any exogenous growth factors for 48 hours prior to all of the following assays. The cells were metabolically labeled for 8 hours with <sup>35</sup>S-cysteine and <sup>35</sup>S-methionine as described [A. W. Opari, M. S. Boguski, V. M. Dixit, *J. Biol. Chem.* **267**, 12424 (1992)]. Cells on 100-mm dishes were lysed on ice in lysis buffer containing 1% NP-40, 50 mM Tris, and 150 mM NaCl in the presence of protease inhibitors [leupeptin (5  $\mu$ g/ml), aprotinin (5  $\mu$ g/ml), soybean trypsin inhibitor (50  $\mu$ g/ml), and pepstatin (5  $\mu$ g/ml)] for 30 min. The cells were then scraped, clarified by centrifugation, and the supernatants incubated overnight with the indicated antibody or chimera (10  $\mu$ g per immunoprecipitation); 50  $\mu$ l of a 50% slurry of protein A-Sepharose were added and the samples were incubated for 1 hour and then washed three times in lysis buffer. Sample buffer containing 2%  $\beta$ -mercaptoethanol was added, the samples were boiled for 5 min, and the eluted proteins were resolved on 10% SDS-polyacrylamide gels. To deplete Eck, we incubated the samples with 20  $\mu$ g of anti-Eck followed by addition of protein A/G-Sepharose. In vitro kinase assays were done as described (8).
7. For immunoblotting, the cells were lysed in lysis buffer containing 1% NP-40, 50 mM Tris, and 150 mM NaCl in the presence of protease inhibitors. Orthovanadate (1 mM) was included for Figs. 1C and 3A. After blocking overnight in 1% bovine serum albumin (BSA) in Tris-buffered saline containing 0.1% Tween (TBS-T) at 4°C, the filter was incubated with anti-Eck (8) or 4G10 antibody to phosphotyrosine (UBI) at a concentration of 1  $\mu$ g/ml. Bound primary antibody was visualized with the ECL kit (Amersham). Reprobing to detect Eck protein was done as described [A. Pandey, D. F. Lazar, A. R. Saltiel, V. M. Dixit, *J. Biol. Chem.* **269**, 30154 (1994)].
8. R. A. Lindberg and T. Hunter, *Mol. Cell. Biol.* **10**, 6316 (1990).
9. V. Sarma, F. W. Wolf, R. M. Marks, T. B. Shows, V. M. Dixit, *J. Immunol.* **148**, 3302 (1992).
10. Angiogenic activity was assayed in the avascular cornea of F344 female rat eyes (Harlan Laboratories, Madison, WI) as described (20). Briefly, each sample was combined with an equal volume of sterile Hydron casting solution (Interferon Sciences, New Brunswick, NJ), and 5- $\mu$ l aliquots were pipetted onto the surface of 1-mm diameter Teflon rods (Dupont Co.) glued to the surface of a glass petri dish. The resulting pellets were air-dried in a laminar hood and refrigerated overnight. Just before implantation, the pellets were rehydrated with a drop of lactated Ringers solution and then placed in a surgically created intracorneal pocket ~1.5 mm from the limbus. Corneas were observed for a period of 7 days; the animals were then perfused with a colloid carbon solution and the corneas removed, flattened, and photographed.
11. J. Folkman and M. Klagsbrun, *Science* **235**, 442 (1987).
12. Chemotaxis was assayed as described (14, 21). Briefly, we prepared chemotaxis membranes (Nucleopore, 5- $\mu$ m pore size) by soaking them sequentially in 3% acetic acid overnight and for 2 hours in gelatin (0.1 mg/ml). Membranes were rinsed in sterile water, dried under sterile air, and stored at room temperature for up to 1 month. Bovine adrenal gland capillary endothelial (BCE) cells, maintained in gelatin-coated flasks in Dulbecco's modified Eagle's medium (DMEM) with 10% FBS were used as target cells. Twenty-four hours before use, BCE were starved in DMEM with 0.1% BSA. Twenty-five microliters of cells suspended at a concentration of  $1 \times 10^6$  cells/ml in DMEM with 0.1% BSA were dispensed into each of the bottom wells. A chemotaxis membrane was positioned on top of the bottom wells, and the chambers sealed, inverted, and incubated for 2 hours to allow cells to adhere to the membrane. Chambers were then reinverted, and 50  $\mu$ l of test medium were dispensed into the top wells and reincubated for an additional 2 hours. Membranes were fixed and stained with Diff-Quick staining kit (Baxter Diagnostics Inc., McGraw Park, IL) to enumerate membrane-bound cells and cells that had migrated through the membrane to the opposite surface.
13. C. Baglioni, in *Tumor Necrosis Factors: The Molecules and Their Emerging Role in Medicine*, B. Beutler, Ed. (Raven, New York, 1992), pp. 425-438.
14. S. J. Leibovich *et al.*, *Nature* **329**, 630 (1987).
15. L. F. Fajardo, H. H. Kwan, J. Kowalski, S. D. Prionas, A. C. Wilson, *Am. J. Pathol.* **140**, 539 (1992).
16. G. Montrucchio *et al.*, *J. Exp. Med.* **180**, 377 (1994).
17. Quiescent HUVECs were then treated with TNF- $\alpha$  (500 U/ml) or TNF- $\alpha$  plus anti-B61 (20  $\mu$ g/ml, 30 min before addition of TNF- $\alpha$  and 3 and 5 hours after addition of TNF- $\alpha$ ) and grown for 8 hours in 1% BSA (Fig. 3A). Eck was immunoprecipitated with anti-Eck (8) and antiphosphotyrosine immunoblotting was done as described (7). Polyclonal antibody to B61 was raised against recombinantly expressed human B61 and then affinity purified.
18. Quiescent HUVECs were treated as in (17) and then metabolically labeled for 8 hours in the presence of 1% BSA. Cell lysates were incubated with anti-B61 (3E6) (2) or anti-Eck (8) for 2 hours at 4°C. Immune complexes were precipitated by the addition of protein A/G-Sepharose, washed three times in lysis buffer, dissolved in SDS sample buffer, resolved by SDS-polyacrylamide gel electrophoresis under reducing conditions, and subjected to autoradiography.
19. H. Shao, L. Lou, A. Pandey, E. B. Pasquale, V. M. Dixit, *J. Biol. Chem.* **269**, 26606 (1994).
20. R. M. Streiter *et al.*, *Am. J. Pathol.* **141**, 1279 (1992).
21. A. E. Koch *et al.*, *Science* **258**, 1798 (1992).
22. We thank AMGEN for providing anti-Eck and anti-B61. We especially thank R. Lindberg for helpful discussions. We acknowledge the assistance of I. Jones and K. O'Rourke in the preparation of this manuscript. Supported by National Institutes of Health grant DK 39255 to V.M.D. and HL 39926 to P.J.P. R.M.M. is supported by Public Health Service grants PO 1A1331890004, P50AR417030003, MO 1RR000420758, and P60AR20557 and is a Pew Scholar in the Biomedical Sciences.

13 October 1994; accepted 23 January 1995

## How Baseball Outfielders Determine Where to Run to Catch Fly Balls

Michael K. McBeath,\* Dennis M. Shaffer, Mary K. Kaiser

Current theory proposes that baseball outfielders catch fly balls by selecting a running path to achieve optical acceleration cancellation of the ball. Yet people appear to lack the ability to discriminate accelerations accurately. This study supports the idea that outfielders convert the temporal problem to a spatial one by selecting a running path that maintains a linear optical trajectory (LOT) for the ball. The LOT model is a strategy of maintaining "control" over the relative direction of optical ball movement in a manner that is similar to simple predator tracking behavior.

Even recreational baseball outfielders appear to know virtually from the moment of bat contact where to run to catch a fly ball. In this task, the ball's approach pattern renders essentially all major spatial location and depth cues unusable until the final portion of the trajectory. Cues such as stereo disparity, accommodation, image expansion rates, and occlusion help to guide final adjustments in the interception path (1, 2). During most of the task, the only usable information appears to be the optical trajectory of the ball (the changing position of the ball image relative to the background

scenery). Conceivably, outfielders could derive the destination from an assumed projected parabolic trajectory, but research indicates that observers are very poor at using such a purely computational approach (3). In addition, factors such as air resistance, ball spin, and wind can cause trajectories to deviate from the parabolic ideal (1, 4).

One proposed model is that outfielders run along a path that simultaneously maintains horizontal alignment with the ball and maintains a constant change in the tangent of the vertical optical angle of the ball,  $\tan \alpha$  (Fig. 1) (5-9). As the ball rises,  $\tan \alpha$  increases, but at a rate that is a function of the running path selected. If the fielder runs too far in (so that the ball will land behind him),  $\partial(\tan \alpha)/\partial t$  will increase. If he runs too far out (so that the ball will land in front of him),  $\partial(\tan \alpha)/\partial t$  will decrease. The fielder can arrive at the correct desti-

M. D. McBeath and D. M. Shaffer, Department of Psychology, Kent State University, Kent, OH 44242-0001, USA.

M. K. Kaiser, Human and Systems Technologies Branch, NASA Ames Research Center, Moffett Field, CA 94035-1000, USA.

\*To whom correspondence should be addressed.

The OAC model is elegant and has some empirical support (6, 7), but it is flawed in several respects. First, the acceleration to be canceled is of  $\tan \alpha$ , not the vertical optical angle  $\alpha$  itself. When  $\partial(\tan \alpha)/\partial t$  is kept constant,  $\partial\alpha/\partial t$  decreases (most noticeably as  $\alpha$  becomes large), so the OAC model requires maintenance of an optical rate of change that is not constant but decreasing. Second, even if we assume that  $\alpha \approx \tan \alpha$ , OAC solutions require a precise ability to discriminate accelerations. Although there is some debate (6, 10), empirical evidence generally indicates that people are poor at such tasks (8, 11). In short, empirical evidence suggests that typical outfielders lack sufficient acceleration discrimination to account for their accuracy in catching fly balls.

Previous work examining the OAC model focused on balls hit directly toward the outfielder. The ball's lateral motion was assumed to be an irrelevant nuisance variable with little impact on catching performance, except possibly to make the task slightly more difficult (5–8). Presumably, having to take into account both vertical and horizontal motion parameters would be as difficult as or more so than accounting for vertical motion alone. Yet outfielders consider balls hit directly at them to be of a different type and to be harder to catch, not easier. We suggest that the case of a ball hit directly at the fielder is a special case (an aligned “accidental view”) of the more general set of balls hit at various angles to either side. Outfielders appear to use their vantage outside the plane of the ball trajectory in a way that simplifies, rather than complicates, determination of ball destination.

stead examined as a unified two-dimensional (2D) image. The geometry of the optical image is shown in Fig. 2, where  $\alpha$  and  $\beta$ , respectively, specify the vertical and lateral optical angles between the ball and its initial optical location (home plate), and  $\Psi$  specifies the optical trajectory projection angle, or the observed angle of ball movement relative to the background horizon. To clarify, if a head-mounted camera were used,  $\Psi$  would be the angle of ball movement on the image. We propose that the outfielder selects a running path that maintains a linear optical trajectory (LOT) for the ball relative to home plate and the background scenery. A LOT is mathematically equivalent to keeping  $\Psi$  constant. As long as  $\tan \alpha$  and  $\tan \beta$  are controlled so as to increase proportionally to each other over time, then  $\tan \Psi$  (and hence  $\Psi$ ) will remain constant ( $\tan \Psi = (\tan \alpha)/(\tan \beta) = \text{constant}$ ). The solution is based on maintenance of balance between vertical and lateral optical angular change and requires no knowledge of distance to the ball or home plate.

If the fielder is running along a path so that the optical trajectory begins to decelerate vertically, it will manifest by curving down toward the fielder's front horizon. If the optical trajectory begins to accelerate vertically, it will manifest by curving up toward the zenith and arcing past the fielder toward his or her back horizon. Thus, maintenance of a LOT allows fielders to accomplish optical acceleration cancellation by "controlling" the shape of the ball trajectory image.

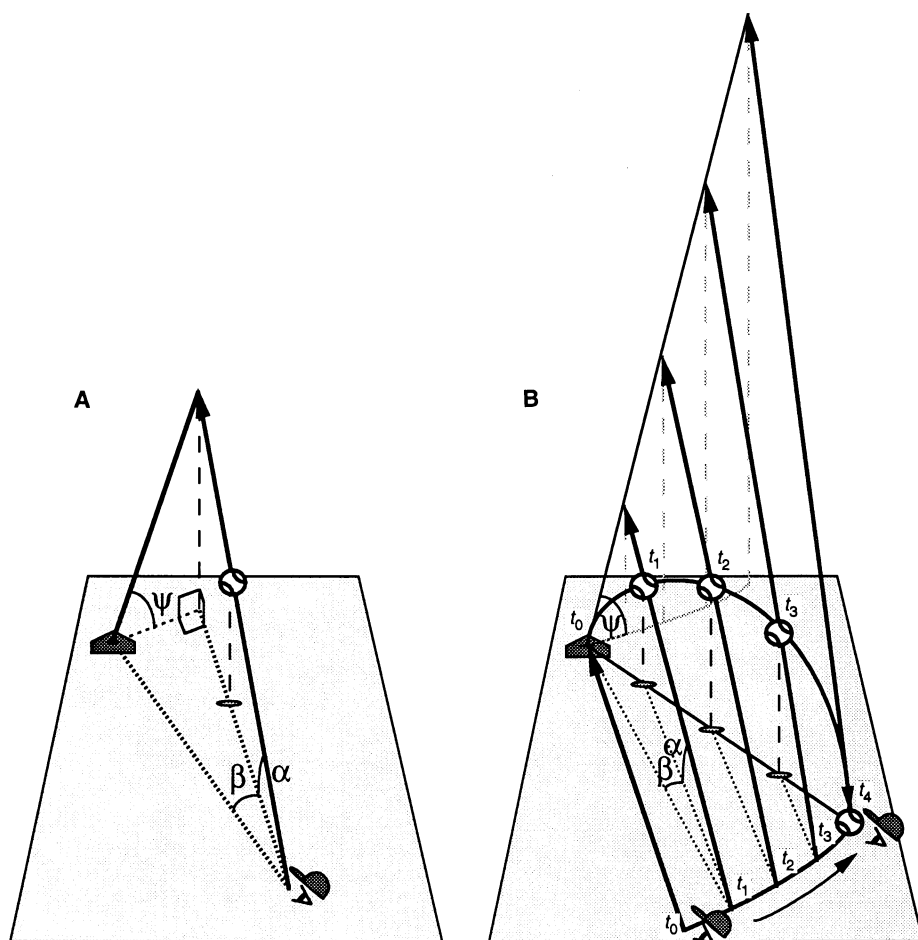
The initial trajectory projection angle  $\Psi$  is fully specified by the lateral angle at which the ball leaves the bat, but maintenance of other, similar projection angles will also work. To maintain a constant  $\Psi$ , the lateral and vertical optical components are not constrained to increase linearly, just proportionally to each other. Yet solutions with nonconstant optical speeds typically result in more running path curvature and more extreme running accelerations. Presumably, fielders would favor LOT solutions close to the one in which the components increase linearly, because solutions in this region keep the running path angle or bearing relatively constant and minimize overall running speed (13).

When a fielder must run to the side and change depth, he or she can maintain a constant increase in the tangent of the lateral optical angle,  $\tan \beta$ , by leading the ball somewhat (scaling his lateral running speed to his distance from home plate). This results in LOT running path solutions in which the

**Fig. 2.** The LOT model. This model specifies that fielders "control" the optical direction of ascent of the ball by adjusting their running path to null optical trajectory curvature. This keeps the image of the ball continuously ascending in a straight line throughout the trajectory. **(A)** Fielder optical angle geometry of a ball at an instant in midflight:  $\alpha$  = vertical optical angle,  $\beta$  = horizontal optical angle, and  $\Psi$  = optical trajectory projection angle (angle from the perspective of the fielder that is formed by the ball, home plate, and a horizontal line emanating from home plate). The configuration of  $\Psi$ ,  $\alpha$ , and  $\beta$  forms a right pyramid such that  $\tan \Psi = (\tan \alpha) / (\tan \beta)$ .  $\alpha$  and  $\beta$  are both controlled to increase continuously throughout the trajectory and are also labeled at time  $t_1$  in **(B)**. **(B)** Bird's-eye view of a fly ball with a running path that maintains a linear optical ball trajectory (positions shown at times  $t_0$  through  $t_4$ ). If the fielder maintains a constant increase in the lateral optical tangent,  $\tan \beta$ , he achieves approximate horizontal alignment with balls that are catchable. When he runs along a path so that both lateral and vertical tangents increase at a constant rate then the trajectory projection angle  $\Psi$  remains constant. Mathematically, the relation is expressed as

$$\tan \Psi = \frac{\tan \alpha}{\tan \beta} = \frac{C_\alpha f(t)}{C_\beta f(t)} = C_\Psi$$

where  $C_\alpha$ ,  $C_\beta$ , and  $C_\Psi$  are constants and  $f(t) = t$  = time since trajectory initiation. In theory,  $f(t)$  could be any monotonically increasing function, but for approximately parabolic trajectories,  $f(t) = t$  leads to a relatively constant bearing and a near least energy running path. The fielder scales lateral running speed relative to his distance to home plate, which generally results in a running path that curves slightly. The resultant optical trajectory is represented behind the ball by the tilted line rising from home plate.



fielder accelerates, curves slightly beyond the ball, and decelerates somewhat as the destination point is approached.

If the ball trajectory deviates somewhat from the parabolic ideal, the LOT strategy still works. Like the OAC strategy, maintaining a LOT is an error-nulling tactic that couples fielder motion with that of the ball. The strategy therefore allows leeway to correct for perceptual error or changes in ball direction due to factors such as ball spin, air resistance, and gusts of wind.

In summary, the OAC model predicts that fielders select a running path that is straight with constant speed, resulting in a curved optical ball trajectory. The LOT model predicts that fielders select a running path that curves out with a  $\cap$ -shaped speed function, resulting in a linear optical ball trajectory.

We ran two experiments to evaluate the OAC and LOT models, each using two college students with some, but not extensive, outfield experience. In the first experiment, we mounted a video camera on a tower above and behind the fielders and videotaped their running paths. Fly balls were launched at a variety of angles at varying force from a distance of about 50 m. To optimize camera angle, balls were aimed so

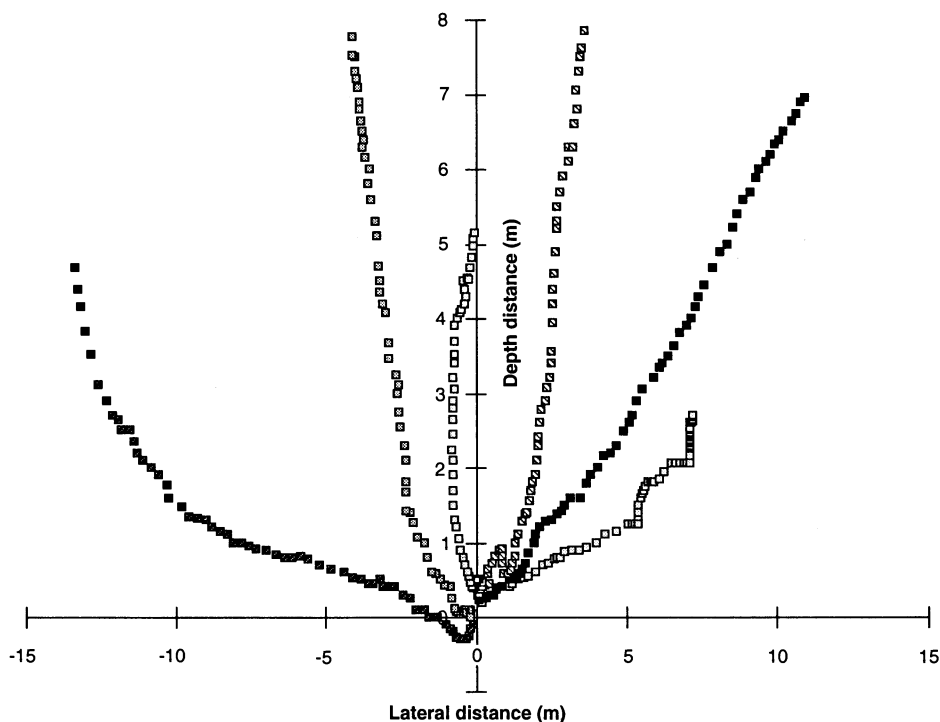


**Fig. 3.** Results of running path experiment. Top view of typical running paths with the origin and similarly patterned squares indicating initial and subsequent fielder positions at 1/30-s intervals. The observed running paths usually curve slightly and vary in speed as predicted by the LOT model.

that fielders ran forward in most trials. We coded 31 trials in which balls were caught. In three trials, the ball was launched directly toward the fielder. These were considered separately because running behavior seemed to be characteristically different, with more backtracking and unsystematic sideways movement. These movements may have been random anticipatory motion or possibly intentional attempts to induce lateral information. More trials of this type need to be examined to make a definitive statement, but our findings are consistent with the notion that these cases are an "accidental view" that may require an alternative strategy. Twenty-eight trials remained in the principal analysis. Distances run to catch fly balls ranged from 2 to 15 m in various directions.

Based on regression analyses, 71% of the running paths curved significantly as predicted by the LOT model ( $z = 5.46$ ;  $P < 0.001$ ) and 75% of the trials varied significantly

in speed as predicted by the LOT model ( $z = 5.89$ ;  $P < 0.001$ ) (Fig. 3). Only 3% of the trials resulted in the constant-speed running behavior predicted by the OAC model. The pattern was the same for balls launched to the right and left. The general pattern of findings suggests that fielders were not maintaining lateral alignment as predicted by the OAC model but rather were circling beyond the ball as predicted by the LOT model.

In the second experiment, we examined the trajectory of the ball from the perspective of the moving outfielder. Here, the fielder carried a video camera on his shoulder that was aimed toward the ball while he ran to make the catch. The fielder stood about 50 m from the launch point, which was in front of a marked wall. Fly balls were launched at a variety of lateral angles at varying forces. In order to facilitate filming, most trials were aimed so that the fielder ran forward. For 31 trials, the fielder both

caught the ball and kept the ball within view of the camera. Four of these trials were considered separately because the ball was launched directly toward the fielder, leaving 27 trials for our analysis. Position of the ball relative to home plate was measured on each video frame to determine both the trajectory projection angle  $\Psi$  and the optical speed of the ball.

Our findings revealed that optical speed exhibited a significant decline in 60% of the cases ( $z = 4.22$ ;  $P < 0.001$ ), refuting the hypothesis that fielders move to maintain a constant optical speed. Yet on median, a linear function accounted for over 99% of the variance of the tangent of the vertical optical angle,  $\tan \alpha$ . This confirms that fielders followed paths consistent with optical acceleration cancellation of  $\tan \alpha$ . Also, on median, a linear function accounted for 97% of the variance of the lateral tangent,  $\tan \beta$ . Thus, the fielders chose paths with lateral change matching the vertical rate. This resulted in the LOT model or linear fit accounting for a median of 96% of the variance of the optical trajectory projection angle  $\Psi$  and additional quadratic curvature for under 2% (Fig. 4). The findings for both running paths and optical trajectories support the LOT model. The outfielders typically selected running paths that circled beyond the ball, had a  $\cap$ -shaped speed function, and maintained a linear optical ball trajectory.

This work supports the premise that outfielders use spatial rather than just temporal cues to initially guide them toward the fly ball destination point. It confirms that optical information can be simplified when analyzed as a full 2D image rather than separated into vertical and horizontal one-dimensional components. We suggest that the act of maintaining a linear trajectory takes advantage of a perceptual invariant—constancy of relative angle of motion—that can be used generically to pursue and approach moving objects (14). Airplane pilots are very accurate at spatial error-nulling tasks and perform particularly well in pursuit tracking tasks with displays that allow them to anticipate and maintain constant angular position relative to a target (15). Predators and organisms pursuing mates commonly adjust their position to maintain control of relative angle of motion between the pair. Tracking research with teleost fish (*Acanthaluteres spilomelanurus*) and houseflies (*Fannia canicularis*) indicates that they follow the motion of their target by maintaining an optical angle that is a function of direction of movement (16). Our findings suggest that baseball players use a similar spatial strategy.

The LOT model explains outfielder behavior well. Once an outfielder establishes a LOT solution, he or she knows he con-

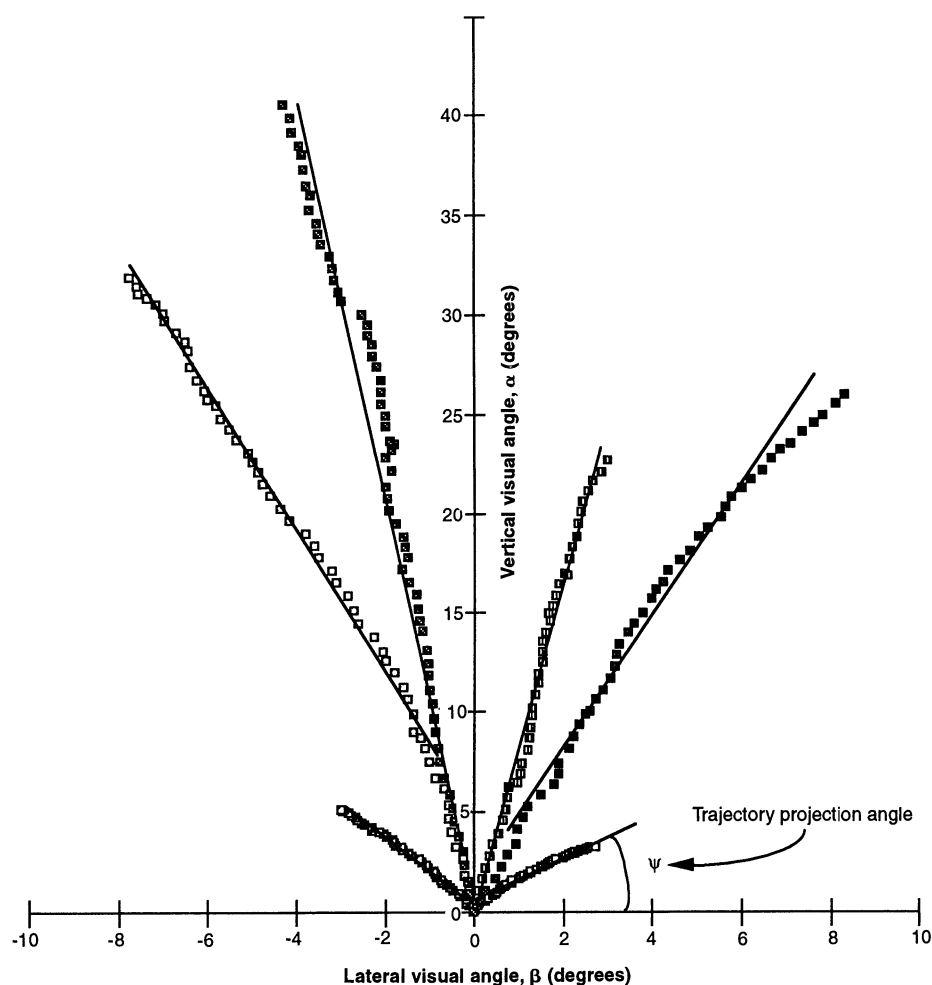


**Fig. 4.** Results of optical trajectory experiment. Fielder's view relative to home plate (origin) for typical examples of optical ball position at 1/30-s intervals up to the last half second. In general, the fielder maintained both vertical and horizontal OAC to achieve a LOT. The two trials that terminate at  $\alpha \approx 5^\circ$  visual angle are line drives, and the other four trials are high fly balls. The few deviations from continuously rising, straight-line trajectories are cases in which the fielder appeared to adjust and initiate a new linear optical direction partway through the trial (as occurred with the leftmost high fly ball shown).

# Potentiated Necrosis of Cultured Cortical Neurons by Neurotrophins

Jae-Young Koh, Byoung J. Gwag, Doug Lobner, Dennis W. Choi\*

trols the situation and will catch the ball, but he does not know when. This explains why fielders run into walls chasing uncatchable fly balls and why they do not rush ahead to the ball destination point, choosing instead to catch the ball while running. The LOT model explains why balls hit to the side are easier to catch. Fielders can use their robust ability to discriminate curvature rather than resorting to their weak ability to discriminate acceleration (11, 12). It is also an error-nulling method that compensates for minor perceptual distortion or flight trajectory irregularity. In short, the LOT strategy provides a simple and effective way to pursue and catch a target traveling with approximately parabolic motion in three-dimensional space.

## REFERENCES AND NOTES

1. M. K. McBeath, *Perception* **19**, 545 (1990).
2. D. Regan, K. I. Beverly, M. Cynader, *Sci. Am.* **241**, 136 (July 1979); D. N. Lee, D. Young, P. Reddish, S. Lough, T. Clayton, Q. J. *Exp. Psychol.* **35**, 333 (1983); G. J. P. Savelsbergh and H. T. A. Whiting, *Ergonomics* **31**, 1655 (1988).
3. B. V. H. Saxberg, *Biol. Cybern.* **56**, 159 (1987a); *ibid.*, p. 177.
4. P. J. Brancazio, *Am. J. Phys.* **53**, 849 (1985); R. K. Adair, *The Physics of Baseball* (Harper and Row, New York, 1990); N. de Mestre, *The Mathematics of Projectiles in Sport* (Cambridge Univ. Press, New York, 1990); R. G. Watts and A. T. Bahill, *Keep Your Eye on the Ball* (Freeman, New York, 1990).
5. S. Chapman, *Am. J. Phys.* **36**, 868 (1968).
6. T. Babler and J. Dannemiller, *J. Exp. Psychol. Hum. Percept. Perform.* **19**, 15 (1993).
7. C. F. Michaels and R. R. D. Oudejans, *Ecol. Psychol.* **4**, 199 (1992); P. McLeod and Z. Dienes, *Nature* **362**, 23 (1993); Z. Dienes and P. McLeod, *Perception* **22**, 1427 (1993); P. McLeod and Z. Dienes, *J. Exp. Psychol. Hum. Percept. Perform.*, in press.
8. J. Todd, *J. Exp. Psychol. Hum. Percept. Perform.* **7**, 795 (1981).
9. J. R. Tresilian, *Perception* **19**, 223 (1990).
10. D. A. Rosenbaum, *J. Exp. Psychol. Hum. Percept. Perform.* **1**, 395 (1975).
11. R. M. Gottsdanker, J. W. Frick, R. B. Lockhard, *Br. J. Psychol.* **52**, 31 (1961); S. Runeson, *Psychol. Res.* **37**, 3 (1974); J. Schmerler, *Perception* **5**, 167 (1976); D. M. Regan, L. Kaufman, J. Lincoln, in *Handbook of Perception and Human Performance*, vol. 1, *Sensory Processes and Perception*, K. R. Boff, L. Kaufman, J. P. Thomas, Eds. (Wiley, New York, 1986), pp. 19.1–19.46; J. B. Calderone and M. K. Kaiser, *Percept. Psychophys.* **45**, 391 (1989).
12. L. A. Riggs, *Science* **181**, 1070 (1973); J. R. Hopkins, J. Kagan, S. Brachfeld, S. Hans, S. Linn, *Child Dev.* **17**, 1166 (1976); R. J. Watt and D. P. Andrews, *Vision Res.* **22**, 449 (1982).
13. M. K. Kaiser and L. Mowafy, *J. Exp. Psychol. Hum. Percept. Perform.* **19**, 1028 (1993).
14. F. M. Toates, in *Control Theory in Biology and Experimental Psychology* (Hutchinson Educational, London, 1975), pp. 151–257; C. D. Wickens, in *Engineering Psychology and Human Performance* (HarperCollins, New York, 1992), pp. 466–481; J. E. Cutting, P. A. Braren, P. M. Vishton, *Psychol. Rev.*, in press.
15. J. A. Adams, *Psychol. Bull.* **58**, 55 (1961); S. N. Roscoe, *Hum. Factors* **10**, 321 (1968).
16. T. S. Collett and M. F. Land, *J. Comp. Physiol.* **99**, 1 (1975); B. S. Lanchester and R. F. Mark, *J. Exp. Biol.* **63**, 627 (1975).
17. Supported in part by a grant from Interval Research Corporation, Palo Alto, CA. We thank S. Krauchunas for camera assistance and K. McBeath for editorial suggestions.

The effects of neurotrophins on several forms of neuronal degeneration in murine cortical cell cultures were examined. Consistent with other studies, brain-derived neurotrophic factor, neurotrophin-3, and neurotrophin-4/5 all attenuated the apoptotic death induced by serum deprivation or exposure to the calcium channel antagonist nimodipine. Unexpectedly, however, 24-hour pretreatment with these same neurotrophins markedly potentiated the necrotic death induced by exposure to oxygen-glucose deprivation or *N*-methyl-D-aspartate. Thus, certain neurotrophins may have opposing effects on different types of death in the same neurons.

Four related members of the neurotrophin family of growth factors have been identified to date: nerve growth factor (NGF), brain-derived neurotrophic factor (BDNF), neurotrophin-3 (NT-3), and neurotrophin-4/5 (NT-4/5) (1). These neurotrophins act on a set of high-affinity receptor tyrosine kinases (2)—TrkA, TrkB, and TrkC—to promote survival, differentiation, and neurite extension in many types of mammalian central neurons. In health, the survival-promoting effects of neurotrophins are probably mediated by the antagonism of naturally occurring programmed cell death. This death generally occurs by apoptosis, characterized by cell volume loss, membrane blebbing, chromatin condensation, and DNA fragmentation (3). Some programmed cell death can be inhibited by transcription or translation inhibitors, which suggests that expression of active “death proteins” is required (4).

Neurotrophins can also attenuate the pathological neuronal death induced by different insults. For example, they inhibit several forms of axotomy-induced death, an apoptotic death that most likely reflects the failure of target-supplied trophic factors to reach the cell body. The degeneration of basal forebrain cholinergic neurons that results from fimbria-fornix lesions can be blocked by administration of BDNF or NGF (5), and the degeneration of axotomized spinal motoneurons can be blocked by administration of BDNF (6).

In addition, neurotrophins (7) as well as other growth factors (8) can reduce the neuronal death induced by exposure to excitotoxins, glucose deprivation, or ischemia. These deaths are thought to occur by necrosis, a process morphologically distinguishable from apoptosis and characterized by prominent early cell swelling (3). Thus, it is widely held that the survival-promoting properties

of neurotrophins are extensive, perhaps involving interference with injury mechanisms common to both apoptosis and necrosis (9).

However, recent studies suggest that apoptosis itself may occur in paradigms involving excitotoxins or oxygen-glucose deprivation. Morphological changes and DNA fragmentation consistent with apoptosis have been described in 3-day-old cultured cortical neurons exposed to glutamate (10) and adult cortical neurons at the periphery of focal ischemic insults in vivo (11). In addition, the protein synthesis inhibitor cycloheximide has been shown to reduce hypoxic neuronal death in rodents and in cortical cultures in which excitotoxicity has been pharmacologically blocked (12). We hypothesized therefore that the neuroprotective effects of neurotrophins may be restricted to apoptosis. To test this, we determined the effects of neurotrophins on murine cortical cell cultures exposed to stimuli that induced apoptosis or necrosis.

To induce neuronal apoptosis, we transferred near-pure neuronal cultures (Fig. 1A) to serum-deficient medium (13), resulting in widespread neuronal degeneration over 24 hours (Fig. 1, B and F). This type of neuronal death showed three features typical of apoptosis. (i) The neurons exhibited gradual cell body shrinkage (Fig. 1B); (ii) death was almost completely abrogated by the addition of cycloheximide (Table 1); and (iii) death was accompanied by the appearance of a DNA “ladder” upon agarose gel electrophoresis (Fig. 1E) (14). Addition of BDNF, NT-3, or NT-4/5 to the bathing medium (all at 100 ng/ml) markedly reduced neuronal degeneration (Fig. 1, C and F). In contrast, NGF did not show any neuroprotective effect (Fig. 1, D and F); a control experiment documented the ability of our NGF sample to rescue PC-12 cells from serum deprivation-induced death (15).

We also induced neuronal apoptosis by exposing mixed neuron-glia cultures to the dihydropyridine calcium channel antagonist nimodipine, which resulted in neuronal de-

Center for the Study of Nervous System Injury and Department of Neurology, Box 8111, Washington University School of Medicine, 660 South Euclid Avenue, St. Louis, MO 63110, USA.

\*To whom correspondence should be addressed.

30 August 1994; accepted 28 February 1995